3-2016

Osteoinductive PolyHIPE Foams as Injectable Bone Grafts

J. L. Robinson

M. A. P. McEnery

H. Pearce

M. E. Whitely

Dany J. Munoz Pinto
Trinity University, dmunozpi@trinity.edu

See next page for additional authors

TISSUE ENGINEERING: Part A
Volume 22, Numbers 5 and 6, 2016

DOI: 10.1089/ten.tea.2015.0370

termis
Tissue Engineering
& Regenerative Medicine
International Society

ORIGINAL ARTICLE

Osteoinductive PolyHIPE Foams as Injectable Bone Grafts

Jennifer L. Robinson, PhD,[1] Madison A.P. McEnery, BS,[1] Hannah Pearce,[1]
Michael E. Whitely, BS,[1] Dany J. Munoz-Pinto, PhD,[2] Mariah S. Hahn, PhD,[2] Huinan Li, BS,[3]
Nicholas A. Sears, MS,[1] and Elizabeth Cosgriff-Hernandez, PhD[1]

We have recently fabricated biodegradable polyHIPEs as injectable bone grafts and characterized the mechanical properties, pore architecture, and cure rates. In this study, calcium phosphate nanoparticles and demineralized bone matrix (DBM) particles were incorporated into injectable polyHIPE foams to promote osteoblastic differentiation of mesenchymal stem cells (MSCs). Upon incorporation of each type of particle, stable monoliths were formed with compressive properties comparable to control polyHIPEs. Pore size quantification indicated a negligible effect of all particles on emulsion stability and resulting pore architecture. Alizarin red calcium staining illustrated the incorporation of calcium phosphate particles at the pore surface, while picrosirius red collagen staining illustrated collagen-rich DBM particles within the monoliths. Osteoinductive particles had a negligible effect on the compressive modulus ($\sim$30 MPa), which remained comparable to human cancellous bone values. All polyHIPE compositions promoted human MSC viability ($\sim$90%) through 2 weeks. Furthermore, gene expression analysis indicated the ability of all polyHIPE compositions to promote osteogenic differentiation through the upregulation of bone-specific markers compared to a time zero control. These findings illustrate the potential for these osteoinductive polyHIPEs to promote osteogenesis and validate future *in vivo* evaluation. Overall, this work demonstrates the ability to incorporate a range of bioactive components into propylene fumarate dimethacrylate-based injectable polyHIPEs to increase cellular interactions and direct specific behavior without compromising scaffold architecture and resulting properties for various tissue engineering applications.

Introduction

Tissue engineered bone grafts combine the healing potential of autografts with the availability of alloplasts to better promote regeneration for patients with a variety of injuries, healing rates, and overall health. Polymerization of high internal phase emulsions (polyHIPEs) is a relatively new method for the production of high porosity scaffolds. Altering compositional and processing parameters results in monoliths with a range of pore sizes, porosities, pore morphologies (open vs. closed), compressive properties, and cure times.[1–11] However, a major challenge in designing functional bone grafts is determining a material composition that promotes ingrowth of surrounding bone and proliferation of cells (osteoconduction), the differentiation of progenitor cells down an osteoblastic lineage (osteoinduction), and osseointegration with the native bone. Various scaffold chemistries and bioactive agents are currently being studied to determine a matrix that presents cues to stimulate osteoblastic differentiation of human mesenchymal stem cells (hMSCs) and promote integration and healing. Extensive research has focused on recombinant growth factors, such as bone morphogenetic proteins (BMPs), for effective osteoblastic differentiation of hMSCs. While these factors are excellent at stimulating osteogenesis, recent clinical studies have reported complications such as ectopic bone formation and inflammation-related fatalities.[12,13] In contrast, natural components of bone such as inorganic minerals and matrix proteins have been shown to induce osteogenic differentiation without the undesired side effects of growth factors.[14–16]

Calcium phosphates (CaP) comprise the primary mineral component of native bone and are commonly utilized in bone tissue engineering to promote osteogenesis. Based on Ca/P ratio, crystallinity, and degree of impurities, a range of bioactivities and degradation rates are achieved with calcium phosphates.[17–21] Hydroxyapatite (HA) has also been utilized extensively in biomaterial research illustrating the potential for calcium phosphates to promote osteogenesis *in vitro*. However, at physiological pH, highly crystalline HA exhibits poor solubility and hinders desired cell responses due to low concentrations of calcium and phosphate ions released.[22] Amorphous calcium phosphate lacks any crystal structure and is resorbed more readily than crystalline HA.[23] For this

[1]Department of Biomedical Engineering, Texas A&M University, College Station, Texas.
[2]Department of Biomedical Engineering, Rensselaer Polytechnic Institute, Troy, New York.
[3]Department of Biology, Texas A&M University, College Station, Texas.

reason, many researchers have investigated the resorption rates of mixed calcium phosphate compositions with different percent crystallinities and assessed the effect on *in vivo* bone regeneration.[24,25] The relative ability of these calcium phosphate minerals to stimulate progenitor cell proliferation and differentiation is dependent on the physiological environment and presentation in the scaffold. In contrast, the demineralized bone matrix (DBM) stimulates bone growth by providing an environment in which invading progenitor and inflammatory cells are stimulated to release trophic cytokines to recruit cells for repair.[26] It has been hypothesized that the demineralization process exposes growth factors and other bioactive molecules, which would otherwise remain inactive in the presence of minerals.[26,27] Work by Pietrzak demonstrated that inorganic minerals reduced hydration of the organic matrix limiting the solubility and thereby bioactivity of growth factors such as BMPs.[28] All three of these bioactive particles have been investigated as potential bone graft additives to confer osteoinductive character to a variety of scaffolds.

A unique attribute of the HIPE system is the ability to introduce small particles that can self-assemble at the pore surface due to their size and surface charge. Emulsions stabilized by solid particles, which adsorb to the oil–water interface rather than a molecular surfactant, are termed as Pickering emulsions.[29] Multiple groups have successfully fabricated and characterized water-in-oil (w/o) Pickering polyHIPEs utilizing both titania and silica nanoparticles.[30–33] The preferential location of self-assembled particles at the pore wall potentially provides a bioactive component for direct contact with encapsulated MSCs for signaling to promote osteoblast differentiation. Furthermore, this methodology promotes the ability to use less of the expensive bioactive particles and still achieve the desired cellular response due to the presentation of the particles at the polyHIPE pore walls. Incorporating both calcium phosphate and DBM into injectable polyHIPEs may provide a rigid foam capable of promoting viability, proliferation, and material-based osteogenesis of hMSCs.

A small number of studies have demonstrated the potential of HA modification of polyHIPE monoliths to guide cellular behavior. Bokhari *et al.* incorporated HA into styrene–divinylbenzene polyHIPEs and illustrated the ability to increase the production of bone matrix glycoprotein osteopontin (OPN) and mineral deposition relative to control specimens.[34] In this work, the HA was added to the aqueous phase rather than the organic phase and thereby relied on adsorption onto the polymer struts for maintenance within the polyHIPE. This weak interaction reduces the effective concentration of particles actually at the pore wall surface over time. Zhou *et al.* reported on pickering biopolymer emulsions stabilized with 1–4 wt% HA particles incorporated into the organic phase that resulted in stable monoliths with 1–50 μm pore sizes.[35] However, these were noninjectable hydrogel grafts with insufficient mechanical properties to withstand physiological loading as a bone graft. A recent study of pickering polyHIPEs fabricated with poly(lactic acid)-grafted HA nanoparticles as the stabilizer in poly(lactic-co-glycolic acid) w/o emulsions showed tunable pore architecture, enhanced mineralization potential, and murine MSC viability as a function of grafted HA concentration.[36] These collective results are promising for use of this emulsion templating technique to fabricate porous materials that promote the desired cell behavior. However, all of this work was conducted on prefabricated monoliths, and the use of nondegradable macromers, poor mechanical properties, toxic diluents, or supraphysiological temperatures precludes their use as injectable bone grafts.

Previously, our laboratory has demonstrated the fabrication of injectable biodegradable polyHIPEs without the need for a toxic diluent and with rapid cure rates at physiological temperature.[7,8,37] This platform technology provides a tunable system for fabricating high porosity scaffolds with properties comparable to the trabecular bone that can be used to fill irregularly shaped defects directly in the surgical suite without the need for prefabrication based on computer-aided design. The present study expands upon our injectable polyHIPE platform technology to fabricate monoliths with osteoinductive character to promote osteogenesis and integration. To this end, amorphous calcium phosphate nanoparticles, HA nanoparticles, and DBM particles were added to the organic phase before fabrication to increase hMSC proliferation and osteogenic potential. Redox-cured polyHIPEs promoted incorporation of particles with a range of hydrophobicities and surface charge due to the quick set times that reduced time allowed for phase separation. The ability to incorporate bioactive particles into the HIPE without affecting emulsion stability and resulting pore architecture was investigated using scanning electron microscopy (SEM). The effect of each osteoinductive agent on the compressive properties of propylene fumarate dimethacrylate (PFDMA)-based polyHIPEs was evaluated. Transmission electron microscopy (TEM) techniques and alizarin red calcium staining were used to illustrate the location of the nanoparticles at the pore surface. Finally, the ability of these particles to promote hMSC differentiation *in vitro* was assessed by quantifying the upregulation of RNA coding for the osteoblast-specific markers runt-related transcription factor 2 (*runx2*), alkaline phosphatase (*ALP*), osteopontin (*OPN*), collagen type I (*Col1a1*), and osteocalcin (*OCN*). Overall, this work highlights the potential of this injectable polyHIPE system to be fabricated with osteoinductive particles to promote osteoblastic differentiation of hMSCs and emphasizes the potential of the polyHIPE scaffold technology to enhance bone regeneration.

Materials and Methods

Materials

Polyglycerol polyricinoleate (PGPR 4125) was provided by Palsgaard. hMSCs were provided by the Texas A&M Health Science Center College of Medicine Institute for Regenerative Medicine at Scott & White through a grant from NCRR of the NIH (Grant No. P40RR017447). All other chemicals were purchased and used as received from Sigma Aldrich unless otherwise noted.

Demineralization and homogenization of rat long bones

Euthanized Sprague Dawley rats were obtained from the tissue share program at the Laboratory Animal Research and Resources facility at Texas A&M University. The demineralization process was adapted from Figueiredo *et al.*[38] Long

hind bones were extracted from the rats, rid of soft tissue using a scalpel and gauze, and the majority of marrow removed with water and compressed air. Bones were soaked in a 1:1 volume chloroform: methanol solution at 1 g bone to 30 mL solution for 3 h. After solvent treatment, bones were washed once with reverse osmosis water, placed in a 0.6 M HCl solution, and stirred for 24 h to decalcify. Residual HCl was then removed by rinsing with water, stirring DBM in freezing water, and placed under vacuum at 40°C overnight. DBM was then blended into smaller pieces and homogenized into particles using a handheld digital homogenizer (IKA T25 digital ULTRA-TURRAX). SEM was utilized to determine relative particle sizes. Visual assessment of micrographs determined particle sizes ranging from 50 to 200 μm.

Macromer synthesis and purification

PFDMA was synthesized and purified in a two-step process detailed in our earlier work.[8] Briefly, the diester 1,2 hydroxypropyl fumarate was synthesized by adding propylene oxide dropwise to a solution of fumaric acid and pyridine in 2-butanone (2.3:1.0:0.033 mol) and refluxing at 75°C for 18 h. Residual reagents were removed by distillation, and the product redissolved in dichloromethane before removing acidic byproducts with washing. The diester product was then dried under vacuum before endcapping with methacrylate groups using methacryloyl chloride in the presence of triethylamine. The molar ratios of the diester, methacryloyl chloride, triethylamine were 1:2.1:2.1, respectively. Hydroquinone was added to the diester to inhibit crosslinking during synthesis at a molar ratio of 0.008:1. The reaction was maintained below −10°C to reduce undesirable side reactions and stirred vigorously under a nitrogen blanket. The macromer was neutralized overnight with 2 M potassium carbonate and residual base removed with an aluminum oxide column (7 Al_2O_3:1 TEA). The integration ratio of methacrylate protons to fumarate protons in the ^{1}H NMR spectra was used to confirm >85% functionalization for all macromers before polyHIPE fabrication. (300 MHz, $CdCl_3$) δ 1.33 (dd, 3H, CH_3), 1.92 (s, 3H, CH_3), 4.20 (m, 2H, $-CH_2-$), 5.30 (m, 1H, $-CH-$), 5.58 (s, 1H, $-C{=}CH_2$), 6.10 (s, 1H, $-C{=}CH_2$), 6.84 (m, 2H, $-CH{=}CH-$). Butanediol dimethacrylate (BDMA) was passed through a column containing alumina oxide using high air pressure to remove the monomethyl ether hydroquinone inhibitor and collected in a round bottom flask. The purified products were stored at 4°C under a nitrogen blanket until used for HIPE fabrication.

PolyHIPE fabrication

Quick-curing redox polyHIPEs were fabricated utilizing a FlackTek SpeedMixer DAC 150 FVZ-K following the method developed in our laboratory.[37] A 70:30 molar ratio of PFDMA:BDMA was utilized to ensure an adequate viscosity to mix with a cell suspension in future studies. Previous studies investigating the cytocompatibility of all polyHIPE components have illustrated good hMSC viability (>85%) at 72 h. The organic phase further comprised 10 wt% PGPR and 1 wt% benzoyl peroxide (BPO) initiator or trimethylaniline (TMA) reducing agent. For osteoinductive polyHIPEs, 2 wt% amorphous calcium phosphate (ACP) nanoparticles (<150 nm nanopowder; Sigma), 5 wt% HA nanoparticles (HA, <200 nm nanopowder; Sigma), or 15 wt% DBM was added to the organic phase. These concentrations reflect the maximum concentration of osteoinductive components that promoted stable HIPE formation. HA and ACP were selected to assess the effect of crystallinity and rate of dissolution on osteogenic differentiation. Previous studies have reported a significant increase in calcium ion release and subsequent osteoclast-mediated resorption rate and new bone formation in response to scaffolds containing ACP compared to HA.[24,25] The aqueous solution of calcium chloride (1 wt%) and deionized water was then added to the organic phase (75% v) in six additions and mixed at 500 rpm for 2.5 min each to promote emulsification. The two HIPEs (BPO and TMA) were mixed at 2500 rpm for 30 s in the SpeedMixer to initiate crosslinking. HIPEs were transferred to either 2-mL microcentrifuge tubes or 15-mL centrifuge tubes and placed in a 37°C aluminum bead bath to facilitate crosslinking overnight.

Pore size characterization

SEM (Phenom Pro; Nanoscience Instruments) was utilized to image all polyHIPEs and determine the effect of the incorporation of osteogenic particles on polyHIPE pore sizes. PolyHIPEs were subjected to vacuum drying for 72 h to remove water before pore architecture characterization. PolyHIPEs cured in 15-mL centrifuge tubes ($n = 3$) were sectioned into thirds, fractured at the center, coated with gold, and imaged in a rastor pattern yielding five images for each of the nine specimens per composition. Pore size measurements were completed on the first 10 pores that crossed the median of each 4000× magnification micrograph. Average pore sizes for each polyHIPE composition are reported ($n = 450$). A statistical correction was calculated to account for nonperfect spherical pores, $h^2 = R^2 - r^2$, where R is the void diameter's equatorial value, r is the diameter value measured from the micrograph, and h is the distance from the center. The average diameter values were multiplied by this correction factor, resulting in a more accurate description of pore diameter.[39]

Compressive testing

The effect of each osteoinductive agent on the polyHIPE compressive modulus and strength was investigated following ASTM D1621-04a. PolyHIPEs cured in 15-mL centrifuge tubes were sectioned into disks with a 3:1 diameter to height ratio using an IsoMet saw (Buehler) and compressed using an Instron 3300 at a strain rate of 50 mm/s. The compressive modulus was calculated from the slope of the linear region, and the compressive strength was identified, after correcting to zero strain, as the stress at the yield point or 10% strain, whichever point occurred first. Reported moduli and strength data were averages of three specimens for each polyHIPE composition.

Alizarin red staining of ACP and HA in polyHIPE

Alizarin red binds to calcium ions and was utilized to visually verify the incorporation of calcium phosphate particles in PFDMA/BDMA films and polyHIPEs. In addition, polyHIPEs were stained after culture in growth media (16.5% fetal bovine serum; Atlanta Biologicals, Premium Select, Lot No. B13018) and 1% L-glutamine (Life Technologies) in

Minimum Essential Media-α (MEM-α; Life Technologies) to assess potential calcium deposition from the media after 1 and 2 weeks. PolyHIPEs of each condition were sectioned to 1 mm width specimens using an IsoMet saw (Buehler). Specimens were incubated for 5 min in 2 w/v% alizarin red in distilled water solution, pH 4.1–4.3. Stained specimens were washed with distilled water 5× to remove any unreacted dye and staining captured with digital micrographs.

Picrosirius red staining of DBM in polyHIPE

Picrosirius red, which stains collagen, was used to both verify that the DBM extraction procedure resulted in a collagen-rich matrix and illustrate the incorporation of DBM in the polyHIPEs. A 1 mg/mL solution of picrosirius red was added to specimens and incubated at room temperature for 30 min. Type I rat tail collagen (Sigma) was utilized as a positive control for the stain. Following staining, specimens ($n = 3$) were rinsed with deionized water 5× and imaged with a digital camera.

TEM of polyHIPEs

TEM was utilized to identify the location of calcium phosphate nanoparticles in the HIPEs. PolyHIPEs were first fixed with 3% glutaraldehyde (Electron Microscopy Science) for 15 min followed by fixation for 30 min with a 1% osmium tetraoxide in deionized water on an orbital shaker. After a successive gradient of ethanol dehydration, polyHIPEs samples were infiltrated with an Eponate 12 resin (Ted Pella) on a rotator overnight. Infiltrated samples were then put in a vacuum oven for polymerization. An ultramicrotome (Dupont Instrument; Sorvell, MT2-B) was utilized to make 70 nm sections that were then placed on a copper grid coated with polyetherimide on both sides. Before imaging, grids were stained with saturated uranyl acetate (Ted Pella) and washed with deionized water. The slot grid was imaged with a JEOL 1200 (Jeol Ltd.) operated at 100 kV. Micrographs were collected at 10,000×, 20,000×, and 30,000× magnifications on a bottom-mounted, 9 MP, slow scan, lens-coupled CCD camera SIA 15C (SIA).

hMSC viability and proliferation on polyHIPEs with ACP, HA, and DBM

Investigation of hMSC viability was conducted to assess cell response to injectable PFDMA-based polyHIPEs with osteoinductive particles. Bone marrow-derived hMSCs were obtained as passage 1 in a cryovial from the Center for the Preparation and Distribution of Adult Stem Cells. Cells were cultured in growth media containing 16.5% fetal bovine serum, 1% L-glutamine, and MEM-α to 80% confluency and utilized at passage 3. For these studies, polyHIPEs were cured in 2-mL microcentrifuge tubes, sectioned into 500 μm thick wafers using the IsoMet® saw, and cut to 8 mm diameter with a biopsy punch. For all *in vitro* studies, polyHIPE wafers were weighed down in the 48-well plate utilizing hollow Teflon weights. Specimens were sterilized for 3 h in 70% ethanol, washed four times with phosphate-buffered saline (PBS), and incubated overnight in basal media supplemented with 40 w/v% FBS at 5% CO_2, 37°C. Cells seeded at a density of 100,000 cells/cm^2 onto the polyHIPE sections in growth media supplemented with 1% penicillin/streptomycin (Life Technologies). Viability at 1 and 2 weeks was assessed utilizing the LIVE/DEAD Assay Kit (Molecular Probes) according to manufacturer's instructions. Briefly, cells were washed with PBS, stained with 2 μM calcein and 2 μM ethidium homodimer-1 for 30 min in 37°C, and replaced with PBS for imaging. Rastor imaging (five images per specimen) was conducted on four specimens ($n = 20$) utilizing a fluorescence microscope (Nikon Eclipse TE2000-S). A Quant-iT™ PicoGreen® dsDNA Assay Kit (Molecular Probes) was utilized to quantify dsDNA to determine the effect of particles on hMSC proliferation at 1 and 2 weeks relative to day 1. PolyHIPE sections were removed from the culture wells and placed in unused wells for the lysis procedure before the PicoGreen assay to ensure only DNA from cells adhered onto the scaffolds was measured. Fluorescence intensity was assessed using a plate reader (Tecan Infinite M200Pro) with excitation/emission wavelengths of 480/520 nm, respectively. Average cell numbers were determined by converting dsDNA values to an individual cell number using 6.9 pg DNA/cell.[40]

Gene expression of bone-specific markers

Osteogenic progression of hMSCs at 1 and 2 weeks was evaluated by quantitative real-time polymerase chain reaction (qRT-PCR) relative to day 0. PolyHIPEs with no particles, 2 wt% ACP, and 5 wt% HA were evaluated with hMSCs cultured in growth media. The goal of this study was to determine the maximum osteogenic response achieved through polyHIPEs fabricated with ACP and HA nanoparticles. Therefore, the concentrations of nanopowders reflect the maximum concentration of osteoinductive components that promoted stable HIPE formation. No particle polyHIPEs with hMSCs cultured in osteogenic media (growth media supplemented with 10 nM dexamethasone, 20 nM β-glycerol phosphate, and 50 μM L-ascorbic acid 2 phosphate) were run to compare the effects of soluble cues in the media with material cues. Gene expression was not evaluated on specimens with 15 wt% DBM in this study. Specifically, gene expression for *runx2*, *ALP*, *OPN*, *Col1a1*, and *OCN* was quantified relative to the housekeeping gene *β-actin*. In brief, mRNA was extracted using the Dynabeads mRNA DIRECT Kit (Ambion, Life Technologies) according to the method described by Munoz-Pinto *et al.*[41] Each polyHIPE specimen was rinsed with 250 μL DPBS for 5 min. Thereafter, 250 μL of the provided lysis binding buffer was added over the sample and incubated at room temperature for 10 min. Following incubation, the polyA-mRNA in the extract was harvested using 20 μL of Dynabeads oligo $(dT)_{25}$ magnetic beads. Directly after the rinsing steps, the polyA-mRNA was released from the Dynabeads in 100 μL of 10 mM Tris-HCl by heating the beads to 80°C for 2 min. Purified mRNA was then stored at −80°C until further analysis.

Proprietary qRT-PCR verified primers for human *runx2*, *OPN*, and *β-actin* were purchased from OriGene and *ALP*, *Col1a1*, and *OCN* were purchased from Qiagen. qRT-PCR was performed on each sample using a StepOne Real-Time PCR system (Life Technologies) and the SuperScript III Platinum One-Step qRT-PCR Kit (Invitrogen, Life Technologies). mRNA levels for each gene of interest were assessed in duplicate for each sample. A total of ~25 ng of polyA-mRNA was loaded per 25 μL of reaction mixture at a total primer concentration of 200 nM. Expression of each

gene of interest was calculated relative to *β-actin* using the $\Delta\Delta C_t$ method and following the analysis described by Munoz-Pinto *et al.*[41]

Statistical analysis

All data are displayed as mean ± standard deviation for each composition. A Student's *t*-test was performed on the compressive, viability, and proliferation data to determine any statistically significant differences between compositions at the respective time points. An ANOVA test with Tukey's HSD *post hoc* analysis was conducted on the gene expression data. For the compression and viability studies, tests were carried out at a 99% confidence interval ($p < 0.01$), whereas the proliferation and gene expression tests were conducted at a 95% confidence interval ($p < 0.05$).

Results and Discussions

Incorporating CaP and DBM particles into polyHIPEs

This work focused on the self-assembly of osteoinductive particles at the polyHIPE pore wall to promote material-based osteogenesis and mitigate many of the risks associated with release of potent growth factors. Self-assembly at the interface allows for surface enrichment of nanoparticle additives at the pore wall, which is vital in ensuring encapsulated hMSCs interact with the bioactive agents. Surface enrichment also permits the use of reduced concentrations and minimizes the impact on bulk properties. Initial scoutings were done to determine the maximum concentration of each osteogenic element that promoted stable HIPE fabrication. PolyHIPEs with a 70:30 molar ratio of PFDMA:BDMA were fabricated with the osteogenic components. This macromer composition was chosen based on its viscosity, which promotes mixing with aqueous solutions for future cell encapsulation studies. Redox-cured polyHIPEs that exhibit quick set times allowed for incorporation of particles with a range of hydrophobicities and surface charge by reducing the time allowed for phase separation. Concentrations of 2 wt% ACP, 5 wt% HA, and 15 wt% DBM were the maximum that could be incorporated without substantial phase separation and were the amounts utilized for the remainder of studies.

TEM imaging and colorimetric staining were conducted to verify the presence of the particles at the surface of the polyHIPE sections to ensure direct contact with encapsulated hMSCs. Figure 1 shows representative micrographs of a 5 wt% HA polyHIPE section compared to no particle control. Single nanoparticles are seen self-assembled at the pore surface and aggregated particles are located in the pore wall. This differing behavior is most likely due to the relatively broad size range of the commercial HA nanoparticles (1–100 nm) with smaller nanoparticles migrating to the emulsion interface and larger nanoparticles aggregating in the pore wall. This is supported by the TEM images and a recent study demonstrating the efficient self-assembly of nanoparticles in the range of 5–10 nm at polyHIPE pore walls.[30,42] Recent scouting studies with smaller MgOH nanoparticles (5–20 nm) in these polyHIPEs have confirmed our hypothesis that smaller particles can self-assemble and pack at the pore surface. Notably for this work, alizarin red staining of calcium ions on polyHIPEs with ACP and HA illustrated the presence of these particles at the surface (Fig. 2B) and confirms the presentation of these minerals to cells adhered to the polyHIPE. PFDMA films with ACP and HA nanoparticles stained with alizarin red resulted in no staining (Fig. 2A). It was hypothesized that the particles dissolved in the PFDMA macromer lack any thermodynamic driving force to self-assemble at the film surface, unlike the HIPE system where the change in hydrophobicities at the pore wall promotes this self-assembly. Therefore, the negative staining on the films compared to the positive staining on the polyHIPEs illustrates the surface enrichment of these particles in the polyHIPEs. The self-assembly of these particles at the pore wall indicates the ability to incorporate a lower concentration of bioactive particles while potentially maintaining cellular response due to the increased surface area of particles at the oil/water interface. Furthermore, polyHIPEs cultured in growth media for 2 weeks exhibited a time-dependent deposition of calcium on the surface of the scaffolds (Fig. 5B). This increased calcium content potentially increases the overall osteoinductivity of all polyHIPEs. Picrosirius red collagen staining was utilized to locate DBM particles within the polyHIPE. Because these particles were larger, visual inspection verified their incorporation. Positive staining of these particles within the polyHIPE indicated that the DBM protocol maintained collagen-rich particles (Fig. 2C).

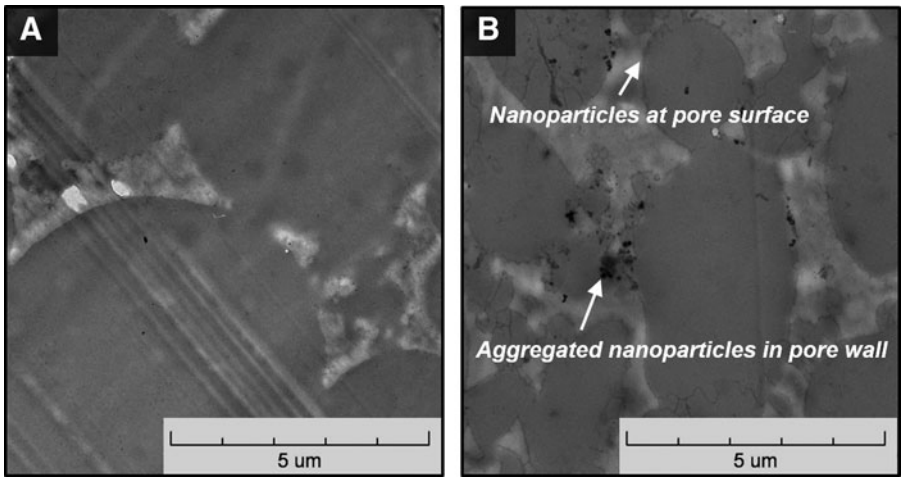

FIG. 1. Transmission electron microscopy (TEM) micrographs of **(A)** polyHIPE control and **(B)** 5 wt% HA polyHIPE show the location of hydroxyapatite nanoparticles both at the pore surface and aggregated within the pore wall.

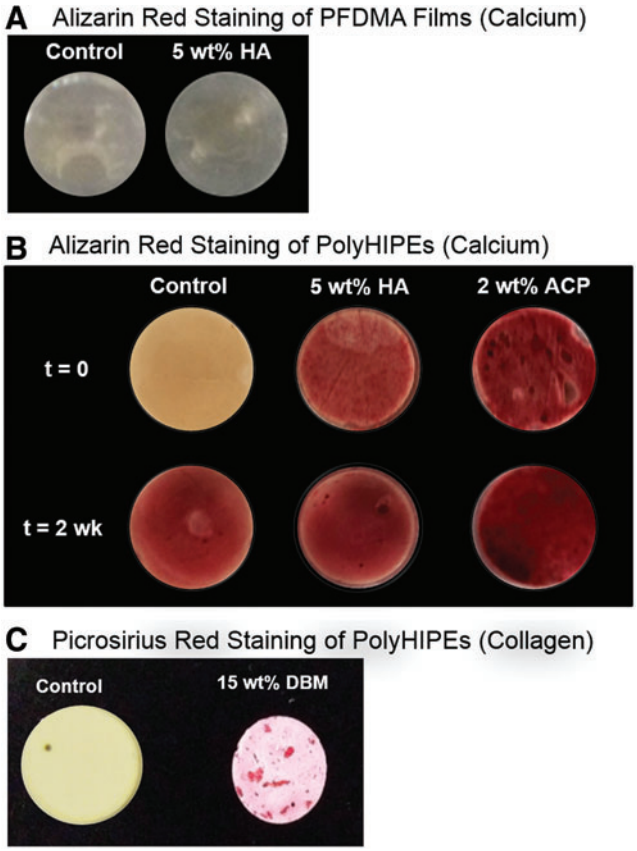

FIG. 2. Particle staining within polyHIPEs and films illustrates the successful incorporation and relative location of the respective particles. Alizarin red was used to stain for calcium ions and picrosirius red used to stain collagen. **(A)** Negative staining of alizarin red of HA nanoparticles in propylene fumarate dimethacrylate (PFDMA) film indicates minimal surface enrichment. **(B)** Alizarin red staining of polyHIPEs cultured in growth media through 2 weeks. All polyHIPEs stained positive for calcium after two weeks, indicating the deposition of calcium from the media. **(C)** Picrosirius red staining illustrating the collagen-rich DBM particles in the polyHIPE. Color images available online at www.liebertpub.com/tea

Fabrication and pore characterization of osteoinductive polyHIPEs

The goal of incorporating osteogenic elements into PFDMA-based polyHIPEs was to confer an osteoinductive character to the grafts without negative impact on the desirable graft properties such as injectability, porosity, and mechanical properties. First, the effect of ACP and HA nanoparticles and DBM particles on pore architecture was assessed. Figure 3 displays the effect of ACP, HA, and DBM on pore architecture. A quantitative assessment of polyHIPE pore size illustrated a negligible effect of ACP, HA, and DBM on HIPE stability at concentrations analyzed as indicated by statistically similar average pore sizes. The ability of the HIPE to fill and cure around the larger DBM particles with minimal gaps is demonstrated in Figure 4. In addition, the maintenance of pore sizes surrounding the DBM particles indicates a negligible effect of these particles on emulsion stability. These results illustrate the ability to incorporate a range of bioactive components to this polyHIPE stystem without altering scaffold architecture.

Compressive properties of polyHIPEs with ACP, HA, and DBM

A potential advantage of using porous PFDMA/BDMA polyHIPEs for bone grafts is their rigid compressive properties. Therefore, it was important to assess the effect of the bioactive agents on the graft compressive modulus and strength. Figure 5 shows the ability to retain the compressive modulus with the incorporation of all particles. These results are further explained with the negligible change in pore architecture, which greatly dictates monolith compressive properties. A slight decrease in compressive strength was observed with the incorporation of ACP, HA, and DBM on polyHIPE, which may be attributed to regions of aggregated particles that may result in stress concentrators within the monolith Figure 1. The ability to incorporate a variety of bioactive agents without affecting pore architecture and resulting compressive properties provides opportunity to design these polyHIPEs for a multitude of tissue engineering applications. Furthermore, it may be possible to modulate cell response in a dose-dependent manner by incorporating a range of concentrations of proteins and inorganic minerals.

hMSC viability and proliferation

Illustrating the ability of these injectable polyHIPEs to promote hMSC differentiation down an osteogenic pathway is one of the major goals of this research. With this in mind, initial verification of hMSC viability on polyHIPE sections is crucial in moving forward with additional cell behavior studies. Two week hMSC viability values after direct

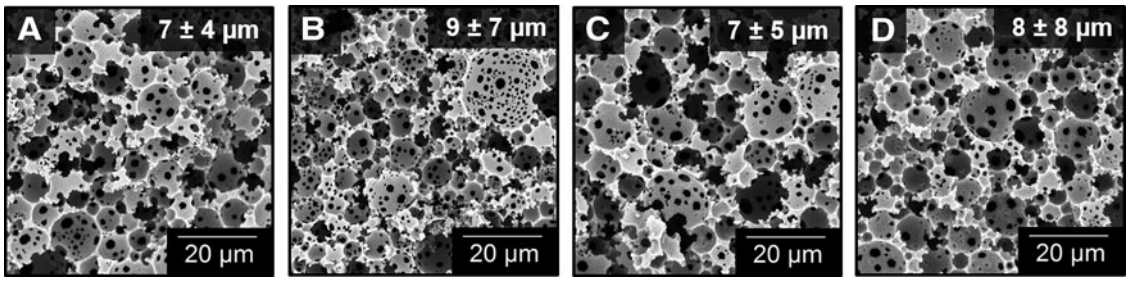

FIG. 3. Representative scanning electron microscopy (SEM) micrographs of **(A)** polyHIPE control, **(B)** 2 wt% amorphous calcium phosphate (ACP), **(C)** 5 wt% hydroxyapatite (HA), and **(D)** 15 wt% demineralized bone matrix (DBM) ($n = 450$) illustrate the effect of osteoinductive particles on pore architecture.

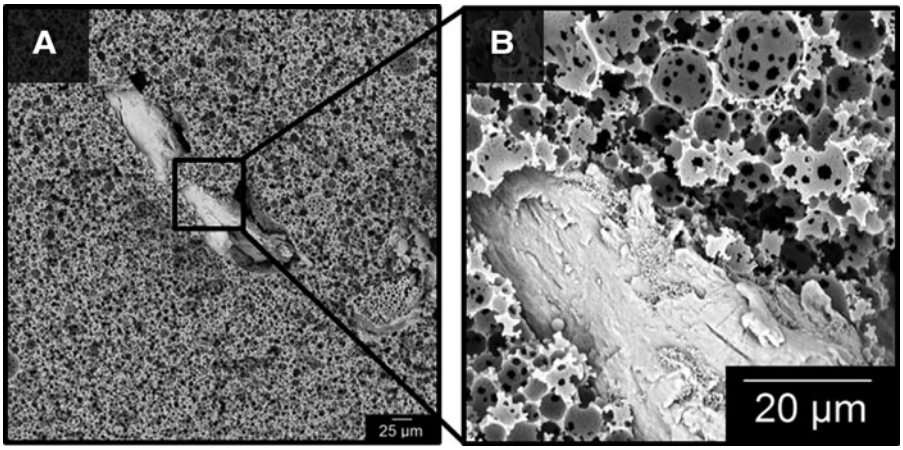

FIG. 4. SEM micrographs illustrate the incorporation of DBM particles with minimal gap at the interface between particle and polyHIPE. Magnification at 500× **(A)** and 4000× **(B)**. PolyHIPE, polymerization of high internal phase emulsions.

culture on polyHIPEs with ACP, HA, and DBM are shown in Figure 6A. All conditions promoted good viability through 2 weeks. Representative images of hMSCs seeded on all polyHIPE compositions at weeks 1 and 2 are shown in Supplementary Figure S1. An increase in cell viability was seen with all bioactive agents compared to the PFDMA/BDMA control at 1 week. PolyHIPEs with ACP, HA, and DBM resulted in greater than 85% viability. This may be attributed to increased cell–cell signaling with the calcium and phosphate ions and enhanced integrin-binding sites from the collagen in the DBM. In addition, the effect of particles on hMSC proliferation is shown in Figure 6B. Proliferation through 2 weeks was observed in all conditions with significant changes in the no particle control and HA polyHIPE groups. Given the fact that it is difficult to promote desired cellular behavior on synthetic materials, this evidence of cell proliferation is promising for future advancements of this material. Furthermore, stable methacrylate-based polyHIPEs with 2 wt% HA and 10 wt% DBM were fabricated illustrating the potential to incorporate multiple bioactive agents to further promote cell adhesion and proliferation. Future work will focus on the effect of polyHIPEs containing both calcium phosphate (various ratios of HA:ACP) and DBM to determine whether there is a synergistic effect. These results highlight the potential of these polyHIPEs to support cellular adhesion and proliferation *in vivo*.

Gene expression of bone-specific markers

Gene expression was evaluated at 1 and 2 weeks to obtain a snapshot of hMSC phenotype after culture on the polyHIPEs as an early indication of osteogenic differentiation. Only the calcium phosphate polyHIPEs were investigated within this study as we focused on osteogenesis through calcium ion stimulation. We hypothesized that the calcium phosphate would stimulate osteogenic differentiation through free calcium ions at a faster rate compared to the no particle control. In the time in which gene expression was sampled, all polyHIPE groups promoted osteogenic gene expression as measured by levels of early osteogenic factors (*runx2* and *ALP*) and later markers (*OCN*, *Col1a1*, and *OPN*) compared to the initial day 0 readings (Fig. 7). As expected, *runx2* and *ALP* levels were generally higher in week 1 compared to week 2. In contrast, *OCN*, *Col1a1*, and *OPN* expressions were all elevated at week 2 compared to week 1. Notably, expressions of these markers for all of the polyHIPEs in growth media were comparable or greater than the control polyHIPE cultured in osteogenic media. This indicates that all compositions displayed an osteoinductive character, but no differentiation between the compositions was observed. There was no significant increase in expression of *runx2*, *ALP*, *OPN*, *Col1a1*, or *OCN* from hMSCs on the polyHIPEs with particles compared to the no particle control.

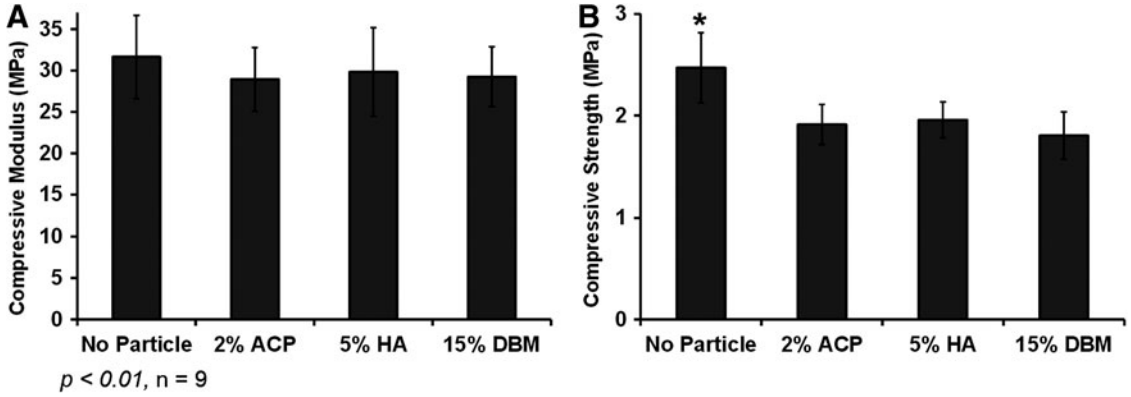

FIG. 5. Effect of osteoinductive particles on polyHIPE compressive modulus **(A)** and strength **(B)**. *denotes the statistical significance between polyHIPE control and polyHIPE with particles.

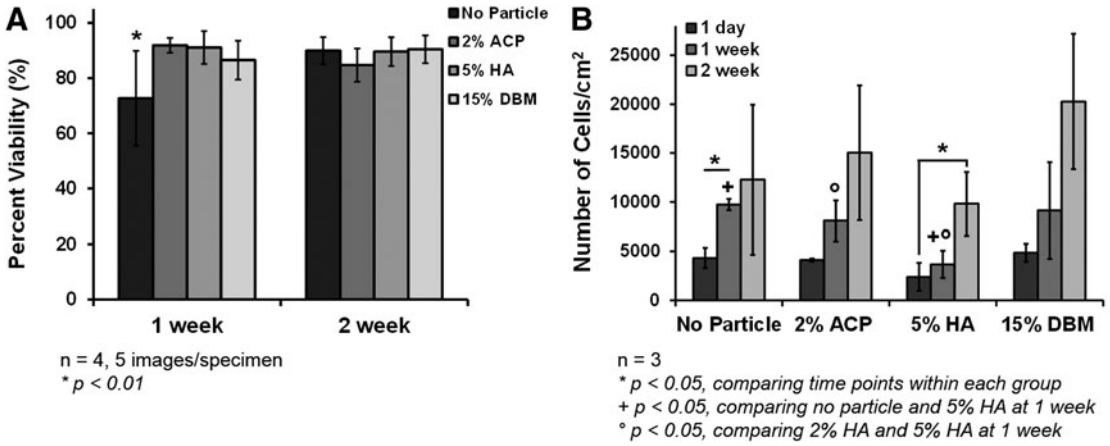

FIG. 6. Human mesenchymal stem cell (hMSC) viability and proliferation on osteoinductive polyHIPEs at 1 and 2 weeks. **(A)** Viability as determined with calcein and ethidium homodimer-1 and **(B)** proliferation determined by DNA quantification measured using a Quant–iT PicoGreen assay. The initial cell seeding density was 100,000 cells/cm^2.

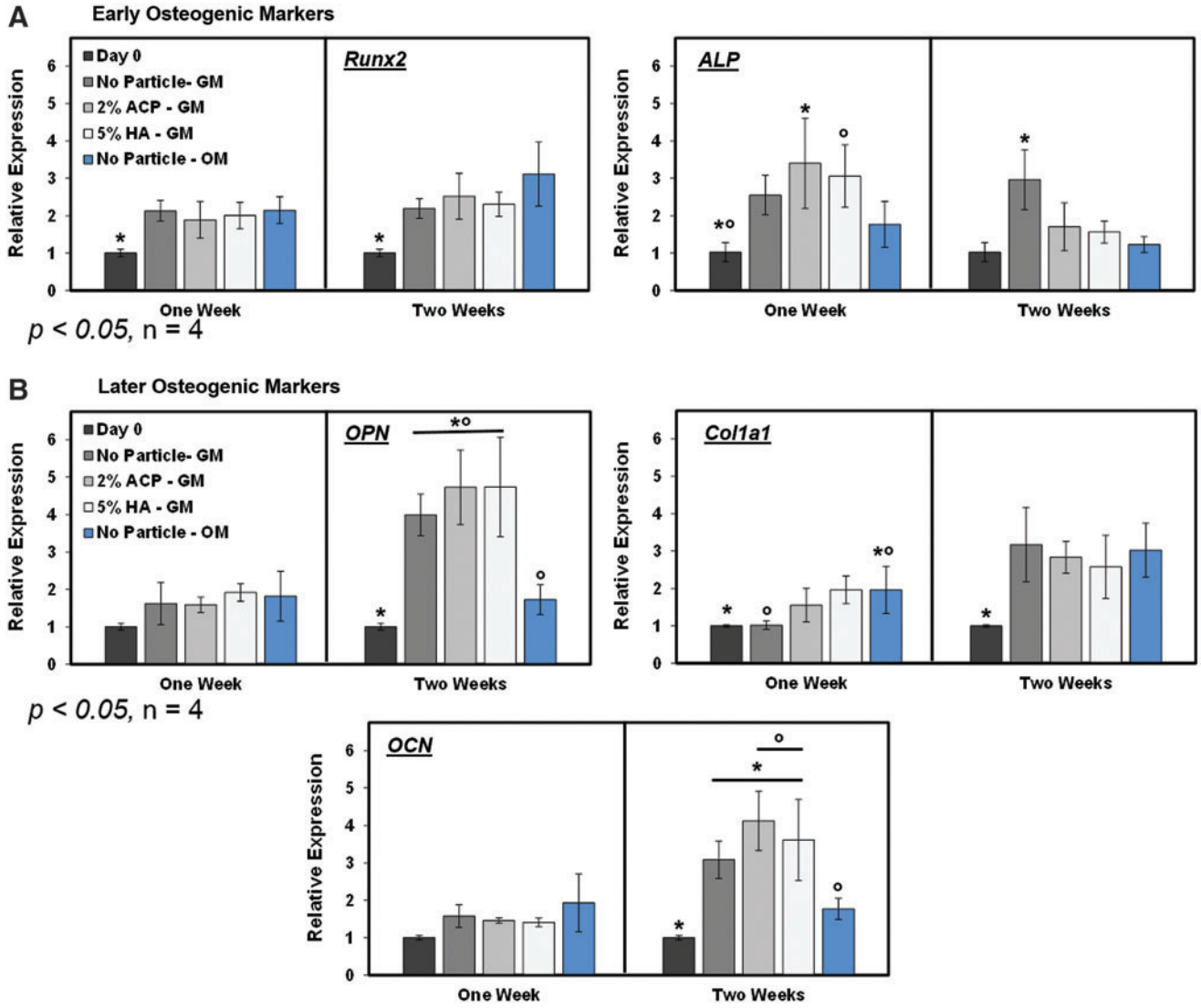

FIG. 7. Gene expression of early and later stage osteogenic markers in growth media and osteogenic media through 2 weeks relative to day 0. hMSCs were cultured on polyHIPEs with no particles, ACP, or HA in growth media (GM) and no particle control polyHIPEs in osteogenic media (OM). **(A)** *Runx2* and *ALP* expression, **(B)** osteopontin (*OPN*), collagen type I (*Col1a1*), and osteocalcin (*OCN*) expression. * indicates significance between marked with an asterisk or all other groups in the case where only one group is marked. o indicates significance between groups marked with the same symbol (o). Color images available online at www.liebertpub.com/tea

Multiple reasons may explain the similar osteogenic gene expression profiles of hMSCs cultured on the no particle controls compared to polyHIPEs with calcium phosphate particles. The most probable reason is the deposition of mineral from the growth media, which resulted in comparable levels of calcium on all polyHIPEs. Figure 5B illustrates positive calcium staining of control polyHIPEs cultured in growth media through 2 weeks in the absence of cells and shows similar stain intensity between all groups. It is probable that the pH and temperature during culture on the polyHIPEs promoted the deposition of calcium to achieve an equilibrium ion concentration. In the body, the process of calcification occurs when the solubility of interstitial calcium is exceeded and is dictated by temperature and pH. Research conducted on rat osteoclasts at pH values ranging from 6.9 to 7.4 indicated that a pH of 7.4 promoted the maximum calcium deposition.[43] Typical basal media are supplemented with buffers to regulate the culture conditions between a pH of 7.2 and 7.4 at 37°C and 5% CO_2. Thereby, these cell culture conditions are ideal for mineralization *in vitro*. This behavior has been seen on other poly(propylene fumarate) (PPF)-based scaffolds with similar chemistries as PFDMA-based polyHIPEs. Specifically, PPF 3D scaffolds have been soaked in simulated body fluid to produce mineralized scaffolds,[44] and PPF-based hydrogels incubated in culture media exhibited increased calcium deposition levels through 28 days in culture.[45]

This deposition of calcium on all polyHIPE compositions may explain the comparable upregulation of bone-specific genes from the seeded hMSCs. Calcium ions are a key regulator in osteoblast cell fate.[46] Higher calcium ion levels are known to stimulate a signaling cascade through the extracellular calcium-sensing receptor, which promotes osteoblast differentiation and inhibits osteoclast differentiation.[47] Many studies have investigated calcium deposition on collagen matrices for tissue engineering applications. Maeno *et al.* investigated the effect of various concentrations of calcium ions in the media on the viability, proliferation, and differentiation of osteoblasts encapsulated in collagen gels. They concluded that 5 mM of calcium ions in the media was optimal for cell survival and differentiation into mature osteoblasts.[48] Studies conducted on collagen sponges in media containing 1.6 mM calcium illustrated minimal calcium deposition on phosphate-free scaffolds compared to 10 wt% calcium deposition on sponges with phosphate indicating the potential role of phosphates as a site of nucleation for mineralization.[49] The basal media utilized in this study contain 1.8 mM calcium plus the calcium found in the fetal bovine serum supplemented to the media. Therefore, we would expect a substantial amount of calcium deposition on the PFDMA-based polyHIPEs in these media conditions. In the body, bone and sera contain 0.8–1.0 and 2.5 mM calcium ions, respectively.[50] In the trabecular bone, 40 wt% of the tissue comprised calcium.[51] Because calcium composes a large fraction of the environment in which these injectable polyHIPEs would be utilized, it is likely that mineral deposition on polyHIPEs *in vivo* would favor osteogenic differentiation of endogenous or encapsulated hMSCs. Ideally, the concentration of calcium phosphate particles incorporated into the polyHIPEs should also promote the deposition of calcium and phosphate ions and enhance hMSC proliferation and differentiation into osteoblasts. However, the high levels of calcium deposition on the control polyHIPE without nanoparticles likely obscured the effects of the nanoparticles and the effect of different dissolution rates of the nanoparticles (HA vs. ACP). Thermal gravimetric analysis and calcium colorimetric assays will be conducted in the future to determine relative concentrations of mineral within the polyHIPE samples to further elucidate dose-dependent effects on hMSC differentiation.

Furthermore, osteogenic differentiation stimulated through soluble factors in the osteogenic media compared to material-based cues from the no particle control polyHIPEs was evaluated. Overall, there was no significant increase in bone-specific gene expression from hMSCs in osteogenic media compared to growth media. In contrast, ALP, OPN, and OCN levels from hMSCs in osteogenic media were significantly lower than expression from cells in the growth media at 2 weeks. This is most likely due to the nature of the test. It is likely that the peak expression of these genes occurred at an earlier time in osteogenic media and was not captured at the time points analyzed. Further investigation should include intermediate and longer time points to better map the gene expression over time for each condition.[52] Once any differences in levels are determined using the altered time points, a systematic study measuring gene expression as a function of particle concentration will be completed. The effect of DBM in the polyHIPE matrix on bone-specific gene expression from hMSCs will also be investigated. Of importance, at the time points we assessed, the expression in normal growth media was comparable to osteogenic media indicating the inherent osteoinductive character of the polyHIPEs. This indicates the strong potential of these grafts to enhance osteogenesis without the need for potent growth factors.

Potential as injectable bone grafts

There has been ongoing research into injectable bone grafts for a wide range of orthopaedic procedures from trauma reconstruction to osteoporotic fracture stabilization.[17,53] Injectable scaffolds that cure *in situ* can fill irregular-shaped defects, enhance scaffold integration with the surrounding tissue, and eliminate the need for costly molding techniques. Current injectable materials are limited by a lack of porosity and biodegradability (e.g., bone cements/putties) or inability to withstand physiological loading (e.g., hydrogels/colloidal gels). A highly porous scaffold that is injectable and cures *in situ* to suitable mechanical strength represents a significant advancement in bone grafting procedures. To this end, we developed a biodegradable polyHIPE composition with rapid *in situ* cure rates and compressive properties comparable to the trabecular bone. We previously demonstrated that the polyHIPE can effectively space-fill an irregularly shaped defect and cure under physiological conditions (37°C and water) with microscale integration with the surrounding bone.[8] Notably, the redox initiation utilized in these grafts does not require external stimuli to initiate crosslinking, which can limit the size of constructs to the effective depth of penetration. Despite these promising findings, there was no confirmation that this new material could support osteoblastic differentiation of hMSCs before this study. This is a critical determinant in the potential utility as bone grafts. Typically, osteogenic differentiation of hMSCs either requires costly

predifferentiation that delays treatment or controlled *in vivo* release of growth factors such as BMP-2. Recent clinical complications due to rapid and uncontrolled release of BMP-2 (e.g., ectopic bone growth, inflammation) have raised safety concerns of this strategy.[12,13] In contrast, the current study demonstrated the ability to modify the surface of the polyHIPE through self-assembly of calcium phosphate nanoparticles at the pore wall without sacrificing desirable graft properties such as injectability, pore architecture, or mechanical properties. Several studies have demonstrated that the presentation of mineral to hMSCs can induce osteogenic differentiation without the negative side effects of supraphysiological levels of growth factors.[15,16] Unexpectedly, osteogenic markers were upregulated in the polyHIPEs with and without the nanoparticles indicating that the base polyHIPE material had an osteoinductive character. We hypothesized that this was due to calcium deposition on the scaffolds from the media and that this effect would translate to the *in vivo* scenario, given the high levels of calcium in bone. A rat calvarial defect study is currently underway to determine the impact of the observed osteoinductive character of the polyHIPE material and any additional benefits of the nanoparticles on osteogenesis. Although the unique combination of properties of these polyHIPEs demonstrates the strong potential as bone grafts, future studies will focus on broadening the pore size and tuning the degradation profile to enhance bone regeneration. In the current studies, a single architecture was investigated with a pore size that is significantly smaller ($\sim 10\,\mu m$) than the typically accepted pore size that promotes cell infiltration and new bone formation (100–400 μm).[54–56] However, we have previously demonstrated that pore size of these injectable polyHIPEs can be readily tuned by altering the stability of the emulsion (surfactant concentration, aqueous phase volume fraction, fabrication conditions) to achieve pore sizes greater than 100 μm.[7,8] Given that our current studies demonstrate that the surface modification had minimal effect on pore size, we expect to be able to utilize this technique to modify polyHIPE grafts with larger pores for investigation as bone grafts in upcoming *in vivo* studies.

Conclusions

ACP, HA, and DBM particles were added to PFDMA-based polyHIPEs to confer osteoinductive character and enhance bone regeneration. To this end, stable HIPEs with each of these bioactive agents were formed with negligible change in pore architecture and compressive properties. Initial hMSC viability testing indicated that all polyHIPE conditions promoted viable cells which proliferated over time on all compositions. Within these studies, we illustrated the inherent ability of PFDMA-based injectable polyHIPEs to promote osteogenic differentiation. Additional work must be done to determine the relative amount of calcium deposition from the media and calcium phosphate nanoparticle resorption rates within the polyHIPE matrix to enhance hMSC osteogenesis. Overall, this work demonstrates the ability to incorporate a range of bioactive components into these injectable polyHIPEs to increase cellular interactions and direct specific behavior without compromising scaffold architecture and resulting properties. There is great translational potential for these rigid porous polyHIPEs as a bone cement material to enhance osseointegration and regeneration.

Acknowledgments

The authors are grateful for the donated materials from Palsgaard and the tissue share program at the Laboratory Animal Research and Resources facility at Texas A&M. hMSCs were provided by the Texas A&M Health Science Center College of Medicine Institute for Regenerative Medicine at Scott & White through a grant from NCRR of the NIH, Grant No. P40RR017447. The authors acknowledge Dr. Mark Harlow for his TEM expertise and resources. Funding for this work was supported by the National Institute for Health (R21 AR057531). In addition, this material is based upon work supported by the National Science Foundation Graduate Research Fellowship Program under Grant No. 2012115842. Any opinions, findings, and conclusions or recommendations expressed in this material are those of the author(s) and do not necessarily reflect the views of the National Science Foundation.

Disclosure Statement

No competing financial interests exist.

References

1. Akay, G., Birch, M.A., and Bokhari, M.A. Microcellular polyHIPE polymer supports osteoblast growth and bone formation *in vitro*. Biomaterials **25,** 3991, 2004.
2. Busby, W., Cameron, N.R., and Jahoda, C.A.B. Emulsion-derived foams (polyHIPEs) containing poly(ε-caprolactone) as matrixes for tissue engineering. Biomacromolecules **2,** 154, 2001.
3. Cameron, N.R., and Sherrington, D.C. Non-aqueous high internal phase emulsions. Preparation and stability. J Chem Soc [Faraday] **92,** 1543, 1996.
4. Kovac?ic?, S., Štefanec, D., and Krajnc, P. Highly porous open-cellular monoliths from 2-hydroxyethyl methacrylate based high internal phase emulsions (HIPEs): preparation and void size tuning. Macromolecules **40,** 8056, 2007.
5. Lepine, O., Birot, M., and Deleuze, H. Preparation of macrocellular PU–PS interpenetrating networks. Polymer **46,** 9653, 2005.
6. Lumelsky, Y., and Silverstein, M. Biodegradable porous polymers through emulsion templating. Macromolecules **42,** 1627, 2009.
7. Moglia, R.S., *et al.* Injectable polyHIPEs as high-porosity bone grafts. Biomacromolecules **12,** 3621, 2011.
8. Robinson, J., Moglia, R., Stuebben, M., McEnery, M.A.P., and Cosgriff-Hernandez, E. Achieving interconnected pore architecture in injectable polyHIPEs for bone tissue engineering. Tissue Eng Part A **20,** 1103, 2014.
9. Williams, J.M. High internal phase water-in-oil emulsions: influence of surfactants and cosurfactants on emulsion stability and foam quality. Langmuir **7,** 1370, 1991.
10. Williams, J.M., and Wrobleski, D.A. Spatial distribution of the phases in water-in-oil emulsions. Open and closed microcellular foams from cross-linked polystryene. Langmuir **4,** 656, 1988.
11. Youssef, C., Backov, R., Treguer, M., Birot, M., and Deleuze, H. Preparation of amazingly hard polyHIPE material from a direct emulsion. Mat Res Soc Symp Proc **1269,** 1, 2010.
12. Perri, B., Cooper, M., Lauryssen, C., and Anand, N. Adverse swelling associated with use of rh-BMP-2 in anterior cervical discectomy and fusion: a case study. Spine J **7,** 235, 2007.

13. Wong, D.A., Kumar, A., Jatana, S., Ghiselli, G., and Wong, K. Neurologic impairment from ectopic bone in the lumbar canal: a potential complication of off-label PLIF/TLIF use of bone morphogenetic protein-2 (BMP-2). Spine J **8,** 1011, 2008.
14. Leupold, J.A., Barfield, W.R., An, Y.H., and Hartsock, L.A. A comparison of ProOsteon, DBX, and collagraft in a rabbit model. J Biomed Mater Res B Appl Biomater **79B,** 292, 2006.
15. Finkemeier, C.G. Bone-grafting and bone-graft substitutes. J Bone Joint Surg **84,** 454, 2002.
16. Van der Stok, J., Van Lieshout, E.M.M., El-Massoudi, Y., Van Kralingen, G.H., and Patka, P. Bone substitutes in the netherlands—a systematic literature review. Acta Biomater **7,** 739, 2011.
17. Bose, S., and Tarafder, S. Calcium phosphate ceramic systems in growth factor and drug delivery for bone tissue engineering: a review. Acta Biomater **8,** 1401, 2012.
18. Ramay, H.R.R., and Zhang, M. Biphasic calcium phosphate nanocomposite porous scaffolds for load-bearing bone tissue engineering. Biomaterials **25,** 5171, 2004.
19. Ducheyne, P., and De Groot, K. *In vivo* surface activity of a hydroxyapatite alveolar bone substitute. J Biomed Mater Res **15,** 441, 1981.
20. Kohri, M., Miki, K., Waite, D.E., Nakajima, H., and Okabe, T. *In vitro* stability of biphasic calcium phosphate ceramics. Biomaterials **14,** 299, 1993.
21. de Groot, K. Bioceramics consisting of calcium phosphate salts. Biomaterials **1,** 47, 1980.
22. Osborn, J.F., and Newesely, H. The material science of calcium phosphate ceramics. Biomaterials **1,** 108, 1980.
23. Popp, J.R., Laflin, K.E., Love, B.J., and Goldstein, A.S. Fabrication and characterization of poly(lactic-co-glycolic acid) microsphere/amorphous calcium phosphate scaffolds. J Tissue Eng Regen Med **6,** 12, 2012.
24. Seol, Y.-J., *et al.* Improvement of bone regeneration capability of ceramic scaffolds by accelerated release of their calcium ions. Tissue Eng Part A **20,** 2840, 2014.
25. Yamada, S., Heymann, D., Bouler, J.M., and Daculsi, G. Osteoclastic resorption of calcium phosphate ceramics with different hydroxyapatite/β-tricalcium phosphate ratios. Biomaterials **18,** 1037, 1997.
26. Urist, M.R. Bone-formation by autoinduction. Science **150,** 893, 1965.
27. Tuli, S., and Singh, A. The osteoinductive property of decalcified bone matrix. An experimental study. J Bone Joint Surg Br **60,** 116, 1978.
28. Pietrzak, W.S. The hydration characteristics of demineralized and nondemineralized allograft bone: scientific perspectives on graft function. J Craniofac Surg **17,** 120, 2006.
29. Pickering, S.U. Emulsions. J Chem Soc **91,** 2001, 1907.
30. Gurevitch, I., and Silverstein, M.S. Polymerized pickering HIPEs: effects of synthesis parameters on porous structure. J Polym Sci A Polym Chem **48,** 1516, 2010.
31. Ikem, V.O., Menner, A., and Bismarck, A. High internal phase emulsions stabilized solely by functionalized silica particles. Angew Chem Int Ed Engl **47,** 8277, 2008.
32. Ikem, V.O., Menner, A., Horozov, T.S., and Bismarck, A. Highly permeable macroporous polymers synthesized from pickering medium and high internal phase emulsion templates. Adv Mater **22,** 3588, 2010.
33. Maeda, H., Okada, M., Fujii, S., Nakamura, Y., and Furuzono, T. Pickering-type water-in-oil-in-water multiple emulsions toward multihollow nanocomposite microspheres. Langmuir **26,** 13727, 2010.
34. Bokhari, M.A., Akay, G., Zhang, S., and Birch, M.A. The enhancement of osteoblast growth and differentiation *in vitro* on a peptide hydrogel—polyHIPE polymer hybrid material. Biomaterials **26,** 5198, 2005.
35. Zhou, S., Bismarck, A., and Steinke, J.H.G. Interconnected macroporous glycidyl methacrylate-grafted dextran hydrogels synthesised from hydroxyapatite nanoparticle stabilised high internal phase emulsion templates. J Mater Chem **22,** 18824, 2012.
36. Hu, Y., *et al.* Facile fabrication of poly(l-lactic acid)-grafted hydroxyapatite/poly(lactic-co-glycolic acid) scaffolds by pickering high internal phase emulsion templates. ACS Appl Mater Interfaces **6,** 17166, 2014.
37. Moglia, R.S. *et al.* Injectable polymerized high internal phase emulsions with rapid *in situ* curing. Biomacromolecules **15,** 2870, 2014.
38. Figueiredo, M., *et al.* Influence of hydrochloric acid concentration on the demineralization of cortical bone. Chem Eng Res Des **89,** 116, 2011.
39. Carnachan, R.J., Bokhari, M., Przyborski, S.A., and Cameron, N.R. Tailoring the morphology of emulsion-templated porous polymers. Soft Matter **2,** 608, 2006.
40. Gregory, T.R. Nucleotypic effects without nuclei: genome size and erythrocyte size in mammals. Genome **43,** 895, 2000.
41. Munoz-Pinto, D.J., Jimenez-Vergara, A.C., Gharat, T.P., and Hahn, M.S. Characterization of sequential collagen-poly(ethylene glycol) diacrylate interpenetrating networks and initial assessment of their potential for vascular tissue engineering. Biomaterials **40,** 32, 2015.
42. Gurevitch, I., and Silverstein, M.S. Nanoparticle-based and organic-phase-based AGET ATRP polyHIPE synthesis within pickering HIPEs and surfactant-stabilized HIPEs. Macromolecules **44,** 3398, 2011.
43. Arnett, T.R. Extracellular pH regulates bone cell function. J Nutr **138,** 415S, 2008.
44. Lan, P.X., Lee, J.W., Seol, Y.-J., and Cho, D.-W. Development of 3D PPF/DEF scaffolds using micro-stereolithography and surface modification. J Mater Sci Mater Med **20,** 271, 2009.
45. Behravesh, E., and Mikos, A.G. Three-dimensional culture of differentiating marrow stromal osteoblasts in biomimetic poly(propylene fumarate-co-ethylene glycol)-based macroporous hydrogels. J Biomed Mater Res A **66A,** 698, 2003.
46. Dvorak, M.M., *et al.* Physiological changes in extracellular calcium concentration directly control osteoblast function in the absence of calciotropic hormones. Proc Natl Acad Sci U S A **101,** 5140, 2004.
47. Marie, P.J. The calcium-sensing receptor in bone cells: a potential therapeutic target in osteoporosis. Bone **46,** 571, 2010.
48. Maeno, S., *et al.* The effect of calcium ion concentration on osteoblast viability, proliferation and differentiation in monolayer and 3D culture. Biomaterials **26,** 4847, 2005.
49. Andre-Frei, V., *et al.* Acellular mineral deposition in collagen-based biomaterials incubated in cell culture media. Calcif Tissue Int **66,** 204, 2000.
50. Forsen, S., and Kordel, J. In: Bertini, I., Gray, H.B., Lippard J., and Valentine, J.S., eds. Bioinorg Chemistry. Calcium in biological systems, Mill Valley, CA: University Science Books, 1994 pp. 107–166.
51. Obrant, K.J., and Odselius, R. The concentration of calcium and phosphorus in trabecular bone from the iliac crest. Calcif Tissue Int **39,** 8, 1986.

52. Gaharwar, A.K., *et al.* Bioactive silicate nanoplatelets for osteogenic differentiation of human mesenchymal stem cells. Adv Mater **25,** 3329, 2013.
53. Kenley, R., *et al.* Biotechnology and bone graft substitutes. Pharmaceut Res **10,** 1393, 1993.
54. Karageorgiou, V., and Kaplan, D. Porosity of 3D biomaterial scaffolds and osteogenesis. Biomaterials **26,** 5474, 2005.
55. Tsuruga, E., Takita, H., Itoh, H., Wakisaka, Y., and Kuboki, Y. Pore size of porous hydroxyapatite as the cell-substratum controls BMP-induced osteogenesis. J Biochem **121,** 317, 1997.
56. Cestro, H.J., Salyer, K.E., and Toranto, I.R. Bone growth into porous carbon, polyethylene, and polypropylene prostheses. J Biomed Mater Res **9,** 1, 1975.

Address correspondence to:
Elizabeth Cosgriff-Hernandez, PhD
Department of Biomedical Engineering
Texas A&M University
5045 Emerging Technologies Building
3120 TAMU
College Station, TX 77843-3120

E-mail: cosgriff.hernandez@tamu.edu

Received: August 19, 2015
Accepted: January 6, 2016
Online Publication Date: February 17, 2016